Proceedings of the
Annual Stability Conference
Structural Stability Research Council
Orlando, Florida, April 12-15, 2016

Revisiting Web Compression Buckling for Wide Flange Sections

Fatmir Menkulasi[1], Nahid Farzana[2], Cristopher D. Moen[3], Matthew R. Eatherton[4]

This paper presents an investigation of the current web compression buckling provisions in AISC specifications section J10.5. The current equations used to check the limit state of web compression buckling were based on beam-column joint tests performed in the 1970s. They were primarily developed to preclude the buckling of the column web in beam column joints of moment resisting connections and were derived based on the elastic buckling of a square panel simply supported on four sides. Accordingly, the width of the applied load is not a variable in the equation. This study proposes a modified equation which accounts for variable load width to section depth ratios. Several wide flange sections are investigated using non-linear finite element analyses to examine their behavior to failure when subject to concentrated loads. For each investigated case a coefficient is provided which can be used together with the proposed equation to more accurately check the limit state of web compression buckling in various loading configurations.

[1]Assistant Professor, Department of Civil Engineering, Louisiana Tech University, Ruston, LA <fmenkula@latech.edu>
[2]Graduate Research Assistant, Department of Civil Engineering, Louisiana Tech University, Ruston, LA, <nahihfarzana303@gmail.com>
[3] Associate Professor, Department of Civil & Environmental Engineering, Virginia Tech, Blacksburg, VA < cmoen@vt.edu>
[4] Assistant Professor, Department of Civil & Environmental Engineering, Virginia Tech, Blacksburg, VA < meather@vt.edu>

1. Introduction

Section J10 of AISC specifications addresses conditions in which flanges and webs are subject to concentrated forces. The limit states addressed in this section are: flange local bending, web local yielding, web crippling, web sidesway buckling, web compression buckling, and web panel zone shear. The provisions for web compression buckling apply to a pair of compressive single-concentrated forces or the compressive components in a pair of double-concentrated forces, applied at both flanges of a member at the same location. Figure 1 provides some examples where the limit state of web compression buckling applies. One example is at a transfer girder in which the column above and the column below align but the girder needs to cantilever over the column below for various detailing reasons. Another example is a beam column moment connection under gravity loads, which features beams framing on both sides of the column. Section J10.5 of the AISC commentary states that under these conditions, the member web must have its slenderness ratio limited to avoid the possibility of buckling. Equation 1 is used to check the limit state of web compression buckling when the pair of concentrated compressive forces is applied at a distance from the member end that is greater than *d/2*, where *d* is the overall depth of the member When this distance is less than *d/2*, a 50% reduction in capacity is recommended, which results in Equation 2. Both, Equation 1 and 2 are valid when the ratio between the load bearing length and overall member depth (*N/d*) is approximately less than 1. When N/d is not small, it is recommended that the member web should be designed as a compression member in accordance with Chapter E of AISC Specifications.

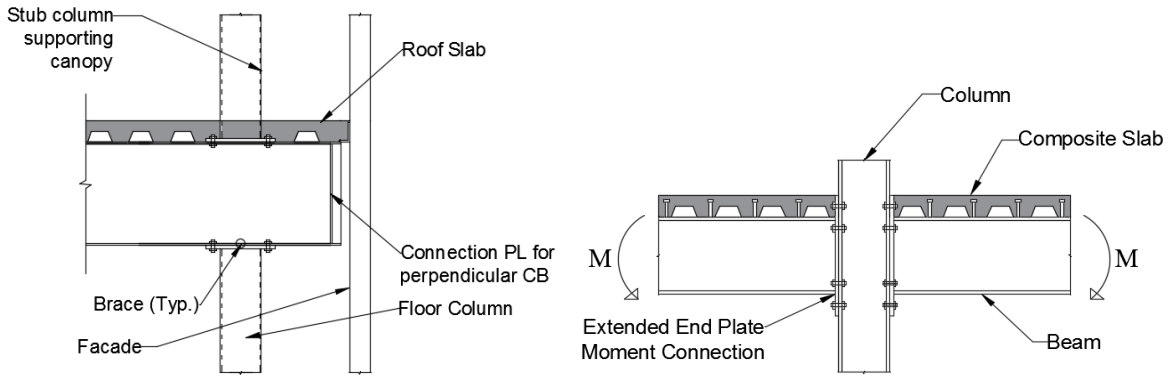

Figure 1. Examples where the limit state of web compression buckling applies

Equation 1 is based on the recommendations of Chen and Newlin (1971) and Chen and Oppenheim (1970), who performed compression tests on several beam sections (Figure 2). These tests were performed to quantify the column web strength in directly welded beam column moment connections (Figure 3 (a)). The pair of concentrated forces illustrated in Figure 2 simulates the compression forces coming from the bottom flanges of the beams. The origin of Equation 1 is the elastic plate buckling equation. It is assumed that the column flange acts as a bearing plate and it distributes the load caused by the beam compression flange of thickness t_b, to some larger length t_b+5k at the edge of the column web. The distance from the column flange to the edge of the column web is defined by *k*, which is the distance from the outer face of the flange to the web toe of the fillet. It is further assumed that the concentrated beam-flange load acts on a square panel whose dimensions are $d_c \times d_c$, where d_c is the clear distance between flanges less the fillet or corner radius (same as *h* in Eq. 1 and 2). The theoretical elastic buckling stress for a plate is provided by

Equation 3. In the case of a square plate simply supported on all four sides, k=4. Additionally, when E=29000 ksi and μ=0.3, Equation 3 reduces to Equation 4. To obtain the critical elastic buckling load for the plate, Equation 4 is multiplied by the thickness (*t*) and the loaded width (*b*) of the plate. This results in Equation 5. Chen and Newlin (1971) proposed Equation 6 to check the limit state of web compression buckling, in which they adjusted the coefficient in Equation 5 to fit the results of the most critical test and introduced the yield stress as a variable. When the yield stress is 50 ksi, Equation 6 reduces to Equation 7. When the modulus of elasticity and yield stress in Equation 1 are taken equal to 29000 ksi, and 50 ksi, respectively, the coefficient becomes 28900, which is the rounded down version of the coefficient provided in Equation 7.

Web Compression Buckling

Away from member ends

$$R_n = \frac{24t_w^3\sqrt{EF_{yw}}}{h} \quad (1)$$

At member ends

$$R_n = \frac{12t_w^3\sqrt{EF_{yw}}}{h} \quad (2)$$

valid for $N/d \leq 1$ (or $d/N \geq 1$)

where

h = clear distance between flanges less the fillet or corner radius for rolled shapes

t_w = web thickness, in.

E = modulus of elasticity of steel (29000 ksi)

F_{yw} = specified minimum yield stress of the web, ksi

N = length of bearing (not less than k for end beam reactions), in.

d = overall depth of the member, in.

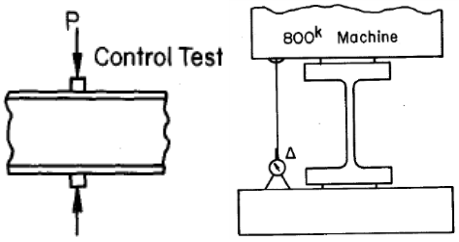

Figure 2: Test setup used by Chen and Newlin (1971) to investigate web buckling strength (reprinted from Chen and Newlin (1971))

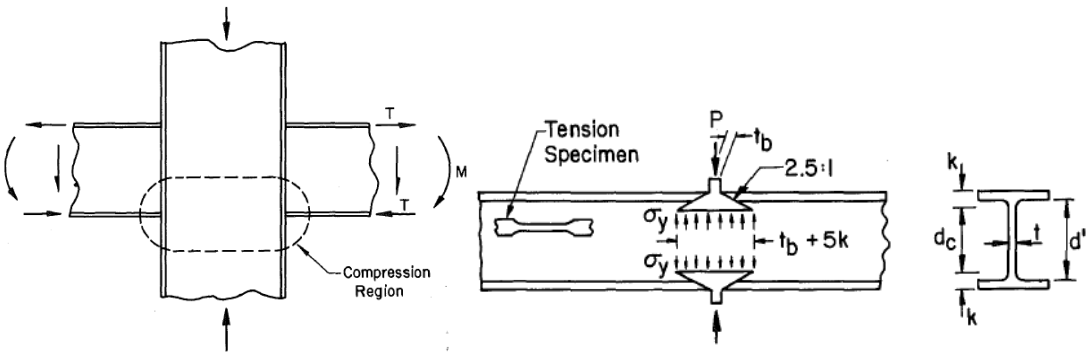

(a) (b)

Figure 3: (a) Schematic of typical interior beam to column connection, (b) Simulation of the compression region (reprinted from Chen and Newlin (1971))

$$F_{cr} = k\frac{\pi^2 E}{12\left(1-\mu^2\right)\left(\frac{b}{t}\right)^2} \tag{3}$$

$$F_{cr} = \frac{104842}{\left(\frac{b}{t}\right)^2} \tag{4}$$

$$P_{cr} = \frac{104842t^3}{b} \tag{5}$$

$$P_{cr} = \frac{4100t^3\sqrt{\sigma_y}}{b} \tag{6}$$

$$P_{cr} = \frac{28991t^3}{b} \tag{7}$$

where

k = constant depending on type of stress, edge support conditions, and length to width ratio (aspect ratio) of the plate.
E = modulus of elasticity
μ = Poisson's ratio
b = with of the plate
t = thickness of the plate

Because Equations 1 and 2 were developed to quantify the column web strength in directly welded beam column moment connections, they may not be applicable to other conditions such as those illustrated in Figure 1. The difference in the case of the transfer girder is clear because the load bearing length provided by the top bearing plate and the bottom cap plate is much larger than the thickness of a beam flange in a directly welded moment connection. Additionally, the applicability of Equation 1 and 2 for other types of moment connections, such as the extended end plate moment connection illustrated in Figure 1 is also questionable. Also, the 50% reduction included in Eq. 2 was introduced in absence of applicable research (AISC 2010). The main shortcoming of Equations 1 and 2 is the fact that the load bearing width is not a variable. Clearly, the greater the load bearing width the greater the portion of the web that can be engaged to resist the applied pair of concentrated compressive forces. Accordingly, the goal of the research presented in this paper is twofold: 1) determine the applicability of current AISC equations for checking the limit state of web compression buckling in a variety of loading conditions, and 2) develop modified equations, which take into account the load bearing width.

2. Research Approach

To investigate the validity of the current AISC provisions for checking the limit state of web compression buckling, a variety of loading cases were investigated. The wide flange sections and depth (h) over loading width (b) ratios that were considered are provided in Table 1 and feature both beam and column sections. The beam sections were selected to represent various bearing type loading conditions for which the limit state of web compression buckling applies. The column sections were selected to represent the loading condition present in beam column moment connections under gravity loading. A total of six beam sections with approximate depths ranging from 8 in. to 30 in were investigated. This range of beam depths covers the majority of wide flange section depths used as beams in steel structures. For each beam section five overall depth over loading width ratios were considered, which ranged from 1.0 to 5.0. Additionally, for each beam

section two loading cases were examined: 1) interior bearing, and 2) end bearing (Figure 4). The loaded length ranges for the beam sections are shown in Table 1. The h/b ratios for the beam sections were selected such that they covered a variety of bearing conditions.

Also, three column sections were investigated with approximate depths ranging from 10 in. to 14 in. The column sections were selected such that they represented the majority of wide flange sections used in column applications. Three overall depth to loading bearing width ratios were considered for the columns and they ranged from 10 to 20. The loaded length ranges for the column sections are shown in Table 1. The h/b ratios for the column sections were selected such that simulate compressive loads coming from beam flanges in moment resisting connections.

Each wide flange section was subject to compressive loads at the top and bottom. The compression load was applied in the form of a uniformly distributed load over the loading bearing length (b) defined in Table 1 through the use of top and bottom plates. The wide flange section was modeled as a deformable body with shell elements. The top and bottom plates were modeled as rigid bodies and were connected to the top and bottom flanges with a tie constraint such that the plates and the corresponding portions of the flanges moved together. The top plate was restrained against translations in directions 1 and 3 and against rotations about all three axis to simulate out-of-plane lateral bracing, the restraint provided by the rest of the beam, and the restraint provided by the slab or any other supported member. The top plate was free to translate in the vertical direction to accommodate the application of the load. The bottom plate was restrained against all translations and rotations.

The length of the wide flange sections was selected such that it was equal to three times the overall depth of the section to allow for a sufficient distribution of the applied load in the web of the section. For example, if the applied load was distributed to the web at a 45^o angle, and the ratio between the overall section depth (h) and the load bearing width (b) is one, then the minimum section length necessary to allow for this distribution is 2h. Accordingly, a section length equal to 3h was chosen in case the distribution of load to the web occurs at smaller angle than 45^o with the horizontal axis. The restraint provided by the continuation of the wide flange section to the vertical edges of the webs was conservatively ignored.

Table 1. Scope of parametric study

Beam Sections	h/b					h/b					Loaded length range (in.)
	1	2	3	4	5	1	2	3	4	5	
W 8×10											1.6 - 7.9
W 12×16											2.4 – 12.0
W 16×31	Interior bearing condition					Exterior bearing condition					3.2 – 15.9
W 21×44											4.1 – 20.7
W 27×84											5.3 – 26.7
W 30×90											5.9 – 29.5

Column Sections	h/b			Loaded length range (in.)
	10	15	20	
W 10×49	Moment Connection			0.5 – 1.0
W 12×65				0.6 – 1.2
W 14×61				0.7 – 1.4

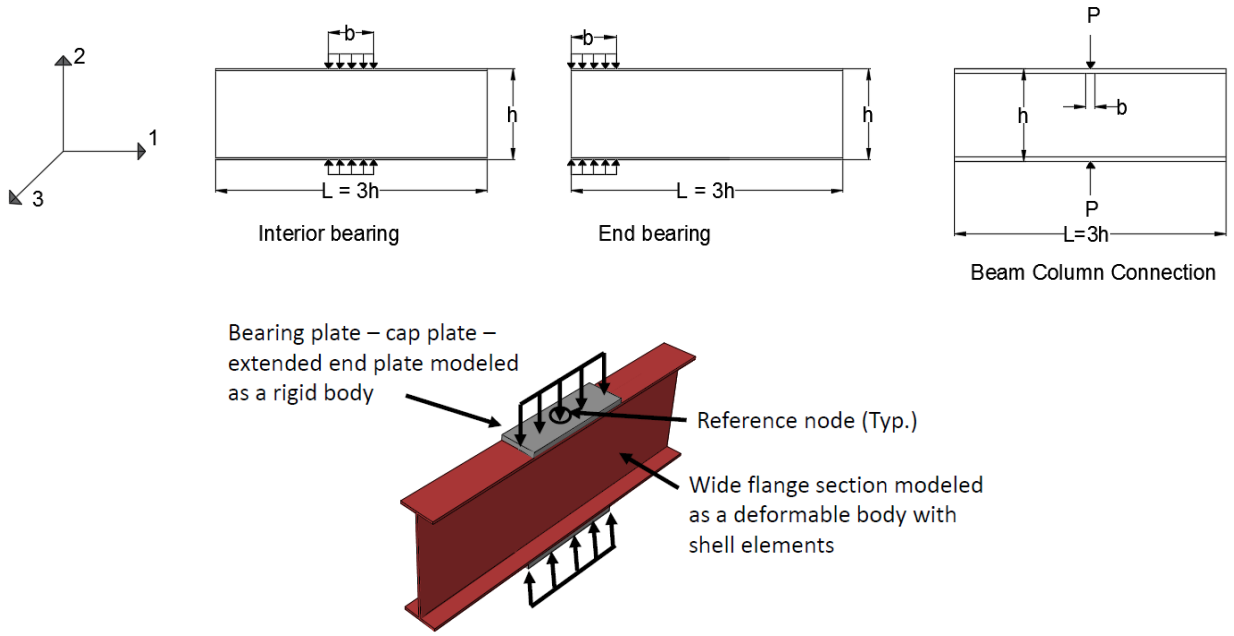

Figure 4: Loading cases and modeling approach considered in the parametric study

A total of 69 nonlinear finite element analyses were performed to obtain failure loads for the investigated specimens and to propose revised equations for checking the limit state of web compression buckling that take into account the influence of the load bearing width. Additionally, failure loads are compared with predicted capacities based on AISC equations for the limit state of web compression buckling.

3. Finite Element Analysis

The numerical simulations described in this paper were performed by using the commercially available finite element analysis software Abaqus (Dassault Systemes 2014). Both flanges and the web were modeled using S8R5 shell elements. The S8R5 element is a doubly-curved thin shell element with eight nodes and it employs quadratic shape functions. The "5" in S8R5 denotes that each element has five degrees of freedom (three translational, two rotational) instead of six (three translational, three rotational). The rotation of a node about the axis normal to the element mid-surface is removed from the element formulation to improve computational efficiency (Moen 2008). The "R" in the S8R5 designation denotes that the calculation of the element stiffness is not exact; the number of Gaussian integration points is reduced to improve computational efficiency and avoid shear locking (Moen 2008). This element is designed to capture the large deformations and through-thickness yielding expected to occur during the out-plane buckling of the web post to failure. The size of the mesh was selected such that each element side did not exceed 1.0 in. in length and was determined based on results from convergence studies to provide a reasonable balance between accuracy and computational expense. It was assumed that the self-weight of the specimens was negligible compared to the applied loads. Although the cross-sections were symmetrical about the major axis, it was necessary to model the full cross-section because the buckled shape could be non-symmetrical.

The finite element model takes into account both material and geometric nonlinearities. The structural steel was modeled using a bilinear stress strain relationship based on coupon test data provided by Arasaratnam et. al (2011). The true stress versus true strain relationship is shown in Figure 5 and was input into Abaqus to define the limits of the Von Mises yield surface. Young's modulus *E*, was set at 29,000 ksi and Poisson's ratio *v*, was set to 0.3. To initiate buckling, an initial small out-of-plane geometric imperfection, in the form of the first mode shape obtained from an eigenvalue buckling analysis, was imposed to the model. An Abaqus.fil file is created for each eigenbuckling analysis, which is then called from the nonlinear.inp file with the *IMPERFECTION command. During the design phase the imperfections are typically unknown and are accounted for in the design equations used to estimate the capacity of the members. They are usually used as general random quantities that can be rigorously treated by stochastic techniques (Soltani et al. 2012). The magnitude of the initial imperfection considered in this study is *h/100*, where *h* is the overall depth of the member. Initial imperfections larger than this magnitude were considered two large to be acceptable. Material nonlinearity is simulated in Abaqus with classical metal plasticity theory, including the assumption of a Von Mises yield surface. In this study residual stresses are not considered.

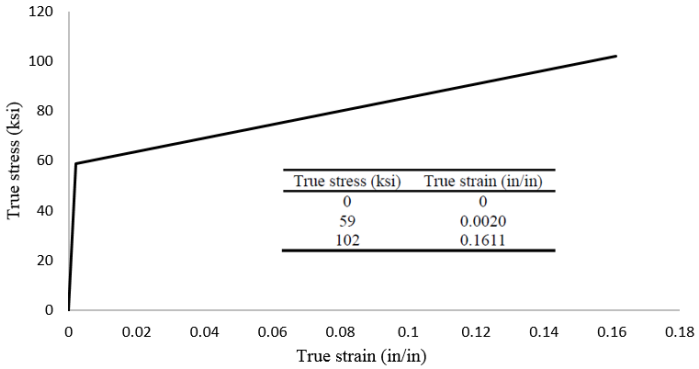

Figure 5: True stress-strain curve based on data from Arasaratnam et al. (2011)

The modified Riks method was used to determine the nonlinear response of the wide flange section. The modified Riks method (i.e.,*STATIC,RIKS in Abaqus), was developed in the early 1980's and enforces an arc length constraint on the Newton-Raphson incremental solution to assist in the identification of the equilibrium path at highly nonlinear points along the load-deflection curve (Crisfield 1981). The loads were applied uniformly along the length of the web. As stated above, the top and bottom plates were modeled as rigid bodies with reference nodes at the centroid of each plate (Figure 4). For each case the vertical displacement of the reference node at the top plate and the reaction at the reference node of the bottom plate were recorded. The maximum vertical displacement at the reference node of the top flange was typically limited to 0.25 in., because such a vertical displacement corresponded with loads that were lower than peak load and were typically well into the descending branch of the load displacement curve.

Figure 6 and Figure 7 show the first buckled mode shapes for W21×44 and W12×65, respectively, for various overall depth (h) to load bearing length (b) ratios. The corresponding elastic buckling loads in terms of uniformly distributed loads obtained from an eigenvalue buckling analysis are also illustrated.

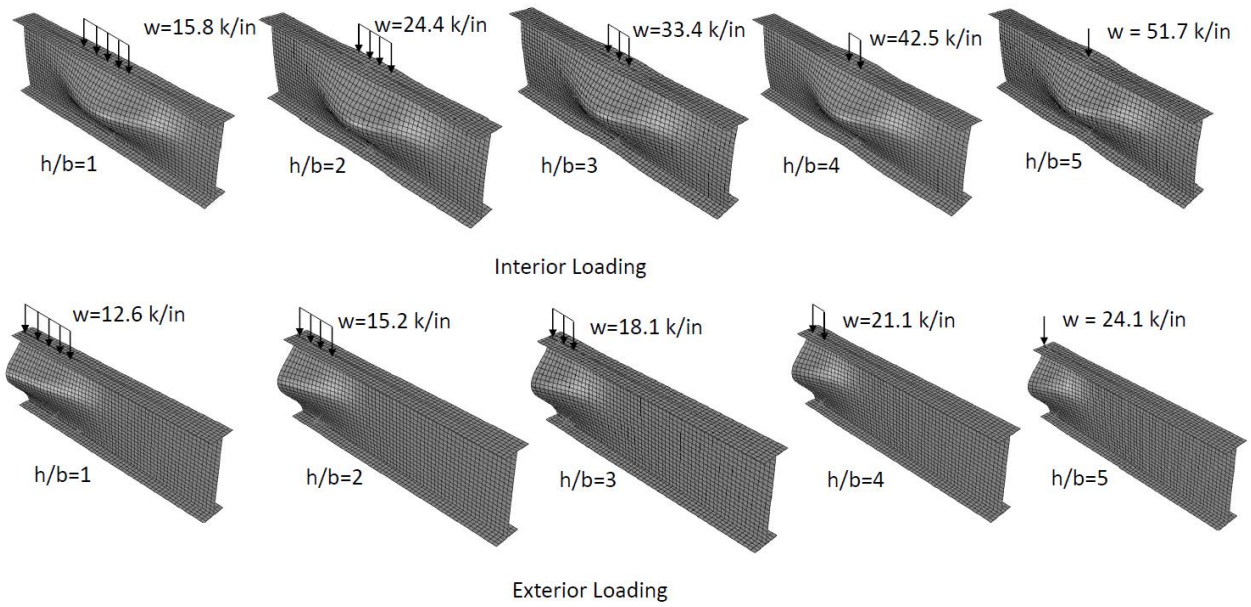

Figure 6. First buckled mode shape for W21×44

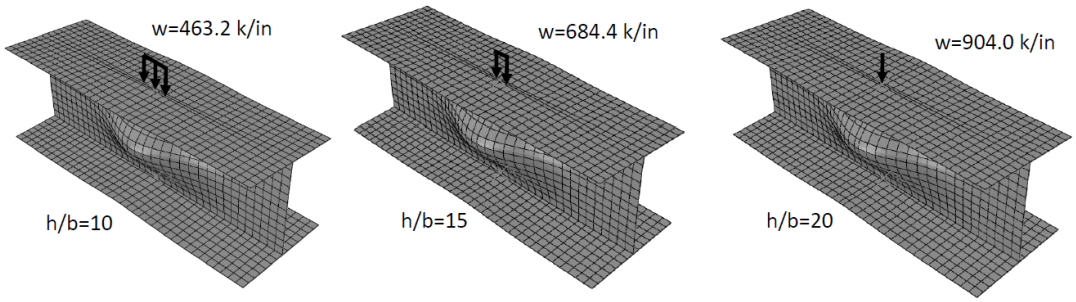

Figure 7: First buckled mode shape for W12×65

Comparison with experimental results

To validate the modeling approach the failure loads for eight beam tests performed by Chen and Oppenheim (1970) and Chen and Newlin (1971) were compared to the failure loads obtained from finite element analyses. The tests were performed on various wide flange sections, which were compressed on both flanges until the web buckled using the test setup illustrated earlier in Figure 2. Table 2 summarizes the wide flange sections and materials properties used in the finite element analyses. Modulus of elasticity (E) and Poisson's ratio were taken equal to 29,000 ksi and 0.3, respectively. The yield stress matched that measured from coupon tests. The ultimate stress and strain were not reported by Chen and Oppenheim (1970) and Chen and Newlin (1971). The ultimate true stress was assumed to be 20% greater than the measured yield stress. The ultimate true strain was assumed to be 0.16.

A summary of the experimentally obtained failure loads and those computed using finite element analyses is provided in Table 3. The average ratio between the peak load obtained from the tests and that obtained from finite element analyses is 1.08. The coefficient of variation is 8.45%. This suggests that the modeling approach used in this study provides reliable results with respect to being able to predict the buckling capacity of the web.

Table 2: Beam sections and material properties used in FEA of tested beams

Test	Section	E (ksi)	ν	σ_y (measured) (ksi)	σ_u (true)	ϵ_u (true)
1*	W 10×30	29000	0.3	41.6	49.92	0.16
2*	W 10×39	29000	0.3	121.9	146.28	0.16
3**	W 12×27	29000	0.3	40.7	48.84	0.16
4*	W 12×30	29000	0.3	39.8	47.76	0.16
5**	W 12×35	29000	0.3	110.6	132.72	0.16
6**	W 12×45	29000	0.3	54 .0	64.8	0.16
7**	W 12×45	29000	0.3	56.8	68.16	0.16
8*	W 12×45	29000	0.3	118.2	141.84	0.16

* Chen and Oppenheim (1970), ** Chen and Newlin (1971)

Table 3: Comparison of failure loads obtained from tests and FEA

Test	Section	$P_{ultTest}$ (kips)	P_{ultFEA} (kips)	Ratio = $P_{ultTest}$/ P_{ultFEA}
1*	W 10×30	90	80.92	1.11
2*	W 10×39	253	231.49	1.09
3**	W 12×27	64	58.83	1.09
4*	W 12×30	61	63.92	0.95
5**	W 12×35	235	191.84	1.22
6**	W 12×45	166	146.17	1.14
7**	W 12×45	168	274.41	0.95
8*	W 12×45	260	152.79	1.10
			Avg.	**1.08**
			COV (%)	**8.45**

* Chen and Oppenheim (1970), ** Chen and Newlin (1971)

4. Results

Load displacement curves and peak loads

Figure 8 shows the applied load versus vertical displacement curves for all beam sections, which were loaded to simulate an interior bearing condition. Table 4 provides a summary of all the peak loads obtained from finite element analyses. As expected, when the loaded length is larger (i.e. h/b ratio lower) the peak load is also larger. This is due to the fact that a larger loaded length engages a greater portion of the web in resisting the applied load, thus resulting in a higher peak load. The difference between the peak loads for h/b ratios equal to 1.0 and 5.0 varies from 50% to 58% for a given section. As can be seen the magnitude of the load bearing length has a significant effect on the buckling capacity of the web. This change in capacity as it relates to the limit state of web compression buckling would have not been captured using the current AISC equation.

Figure 9 illustrates the applied load versus vertical displacement curves for all beam sections, which were loaded to simulate an end bearing condition. Also, in this case the peak loads increase as the loaded bearing length increases. As expected, the peak loads for bearing conditions at the end of the beam are lower than those obtained for a bearing condition at the interior of the beam. This difference becomes more pronounced for higher h/b ratios. For example, the difference between the peak loads obtained for interior bearing and end bearing conditions for a W16×31, when the h/b ratio is equal to 1.0, is 24%. However, when the h/b ratio for the same section is 5.0, the difference in the peak loads is 213%. This is due to the fact that the difference between the portions of the web that are effective in resisting the applied loads is smaller when the loaded bearing length is large. The effective width used in providing resistance to the applied loads consists of the loaded bearing length plus an additional portion of the web, which is engaged in

resisting the load due to the lateral distribution of the load in the web. When the load bearing length is small, then the majority of the effective web width comprises of the portion of the web that is engaged due to the lateral distribution of the load. For an end bearing condition the portion of the web engaged in resistance is half of that used for an interior bearing condition. This is why the peak loads for end bearing conditions are approximately half of those for interior bearing conditions when h/b = 5.

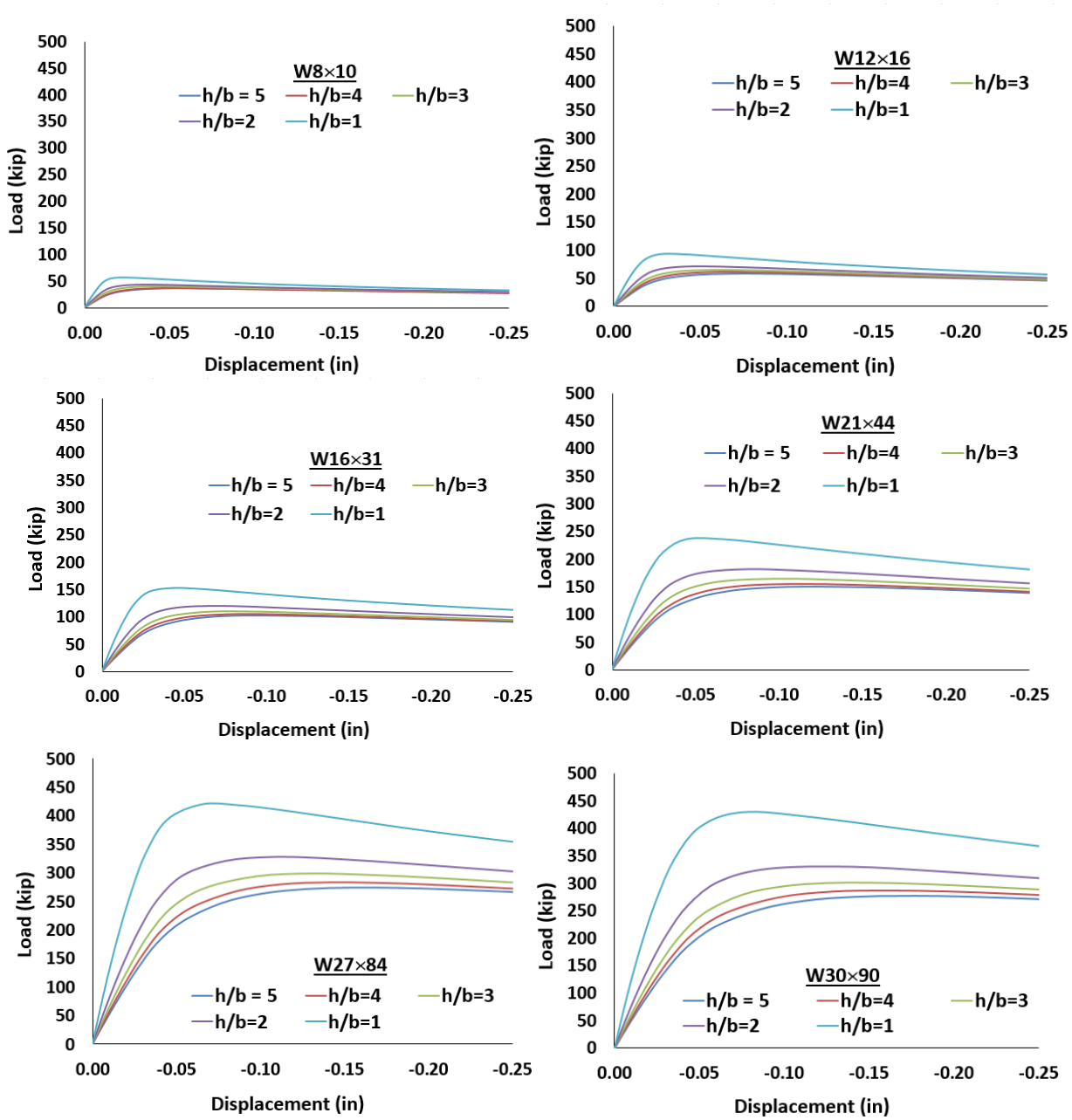

Figure 8: Total load versus vertical displacement at the top of the web (end bearing)

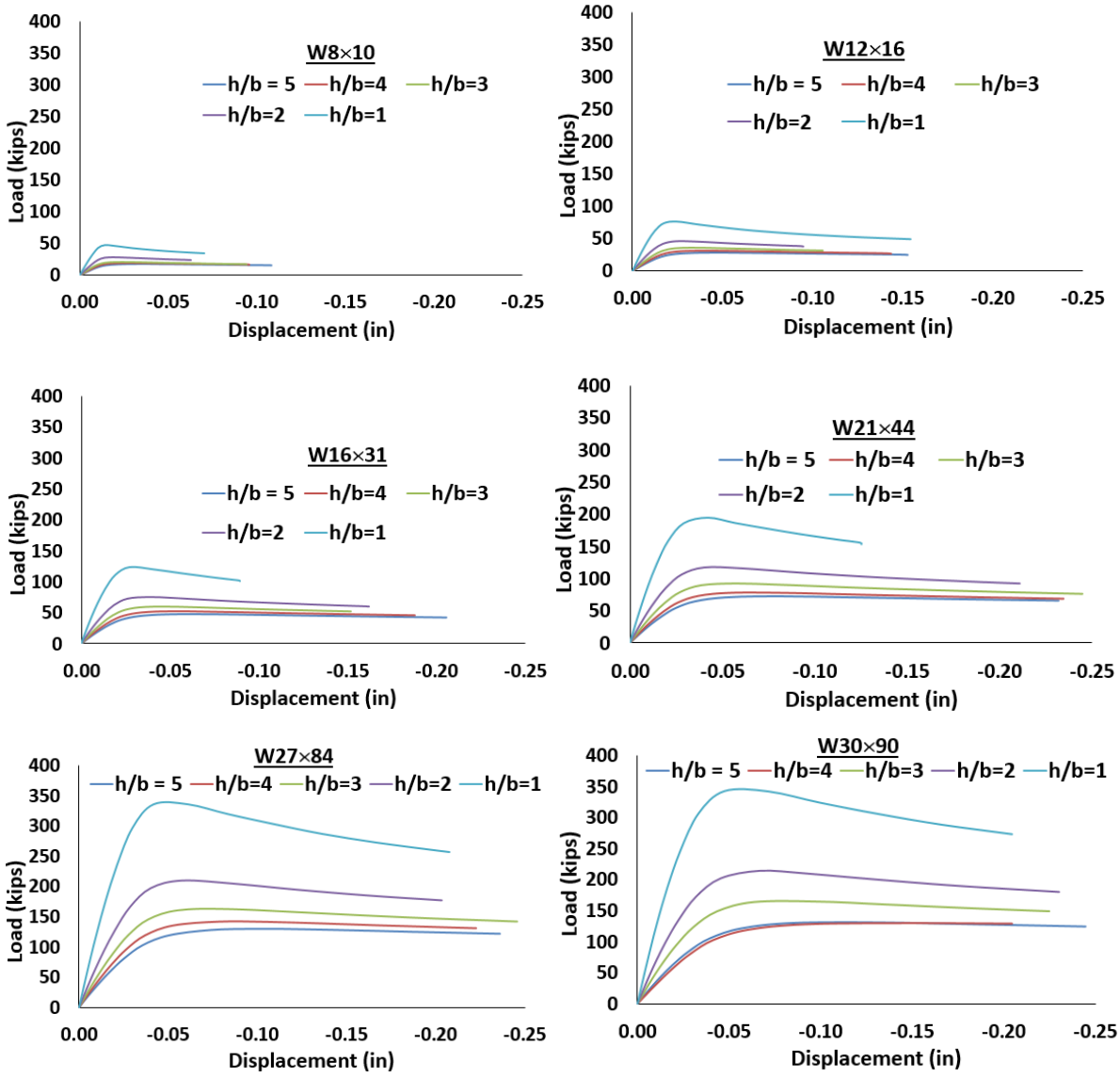

Figure 9. Total load versus vertical displacement at the top of the web (exterior bearing)

Figure 10 shows the load versus vertical displacement curves for the column sections. The column depths considered varied from approximately 10 in. to 14 in. As stated earlier, the column sections represent typically used wide flange sections in column applications. For the column sections the distinction between the peak loads for various h/b ratios is not as pronounced. This is due to the fact that the difference between the loaded lengths is not as pronounced as the one considered for the beam sections. For example, in the case of W12×65 an h/b ratio equal to 20 corresponds to a loaded length equal to 0.6 in. When the h/b ratio is 10 then the loaded length is 1.2 in. Accordingly, a difference between a 0.6 in and 1.2 in loaded length did not result in a marked difference in the peak loads obtained from finite element analysis. The h/b ratio for the columns sections were selected such that they resulted in loaded lengths, which represent concentrated loads coming from beam flanges in moment resisting connections.

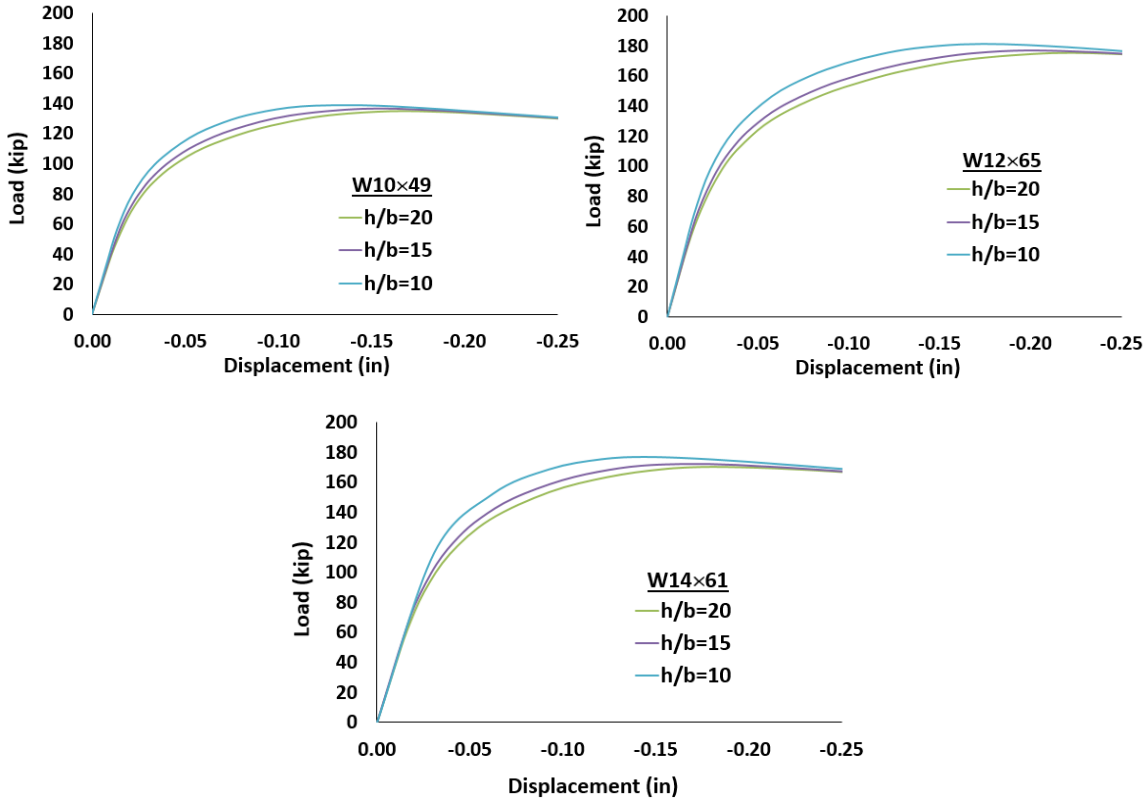

Figure 10: Total load versus vertical displacement at the top of the web (interior bearing)

Table 4. Peak loads (kips)

Beam Sections	h/b (interior) 1	2	3	4	5	h/b (exterior) 1	2	3	4	5
W 8×10	57	44	40	38	36	47	28	20	19	18
W 12×16	92	71	64	61	59	76	46	36	31	28
W 16×31	153	120	110	106	102	123	76	59	52	48
W 21×44	236	182	164	156	151	195	118	92	79	72
W 27×84	420	327	299	284	275	336	209	163	141	130
W 30×90	429	331	302	287	278	342	214	165	144	131

Column Sections	h/b (columns) 10	15	20
W 10×49	139	136	135
W 12×65	181	177	175
W 14×61	177	172	170

Comparison with AISC equations

The peak loads obtained from finite element analyses were compared with predicted capacities based on AISC provisions for the limit state of web compression buckling. The results are presented in Tables 5 through 7. Because the AISC equations (Eq.1 and 2) do not distinguish between various loaded lengths only one prediction is provided for all h/b ratios. The variable *h* in Equations 1 and 2 is defined as the clear distance between flanges less the fillet or corner radius for rolled shapes. Because the wide flange sections in this study were modeled using shell elements for the top and bottom flanges as well as for the web, the variable *h* was taken equal to the distance between the centerlines of top and bottom flanges to make a consistent comparison with the peak loads obtained from finite element analyses.

As can be seen, the AISC equations significantly underestimate the buckling capacity of the web for the beam sections. The ratios between the predicted capacities and computed capacities show that this underestimation becomes more pronounced as the h/b ratios become smaller. This

is expected because higher h/b ratios are closer to the assumption of a simply supported square panel used in the derivation of Equation 1. However, even for h/b ratios equal to 5 the AISC equation still significantly underestimates the buckling capacity of the web. Depending on which beam is considered the underestimation of the buckling capacity for an interior bearing condition and an h/b ratio equal to 5 varies from 45% to 59%. The underestimation of the buckling capacity becomes more pronounced as the section depth gets larger. For h/b ratios higher than or equal to 3.0 the ratios between the predicted capacity and computed capacity for interior and exterior loading conditions are similar. This justifies the 50% reduction for end bearing condition included in Eq.2, however the coefficients 24 and 12 in Equations 1 and 2, respectively are approximately half of what they should be if the predicted load were to match the computed one. For h/b ratios equal to 1 and 2 the ratios between the predicted and computed capacities for end bearing conditions are lower than those calculated for interior bearing conditions. This suggests that the 50% reduction for these h/b ratios is significantly conservative.

Table 7 provides a summary of the predicted capacities and computed capacities for the column sections. Equation 1 was used to predict the web compression buckling capacity of the column webs. The ratios between predicted capacities and computed capacities suggest that Eq.1 does a reasonably good job at predicting the buckling capacity of the column web for sections W10×49 and W12×65. For section W14×61, the prediction of Equation 1 errs on the conservative side by 26-30%. Because the h/b ratios considered for the column sections result in loaded lengths that do not vary as much as those considered in the beam sections, the predicted versus computed ratios for a given section are similar.

Table 5: Comparison of nominal resistance for the limit state of web compression buckling (interior beam bearing)

Beam Sections	P_{nAISC} (kips)	P_{nFEA} (kips) h/b					Ratio= P_{nAISC}/P_{nFEA} h/b				
		1	2	3	4	5	1	2	3	4	5
W 8×10	20.07	56.90	43.96	39.68	37.88	36.32	0.35	0.46	0.51	0.53	0.55
W 12×16	28.49	92.36	70.95	64.22	60.84	58.67	0.31	0.40	0.44	0.47	0.49
W 16×31	42.23	153.19	120.17	110.39	105.52	102.14	0.28	0.35	0.38	0.40	0.41
W 21×44	66.47	235.81	181.65	164.42	156.08	150.61	0.28	0.37	0.40	0.43	0.44
W 27×84	117.26	419.85	327.17	298.68	284.25	274.68	0.28	0.36	0.39	0.41	0.43
W 30×90	112.82	429.24	330.82	301.78	286.91	277.55	0.26	0.34	0.37	0.39	0.41

Table 6: Comparison of nominal resistance for the limit state of web compression buckling (end beam bearing)

Beam Sections	P_{nAISC} (kips)	P_{nFEA} (kips) h/b					Ratio = P_{nAISC}/P_{nFEA} h/b				
		1	2	3	4	5	1	2	3	4	5
W 8×10	10.03	47.28	28.39	20.21	19.27	17.64	0.21	0.35	0.50	0.52	0.57
W 12×16	14.24	76.43	46.14	35.88	30.83	28.33	0.19	0.31	0.40	0.46	0.50
W 16×31	21.12	123.18	76.06	59.33	52.15	47.57	0.17	0.28	0.36	0.41	0.44
W 21×44	33.23	194.60	118.06	91.83	78.76	72.25	0.17	0.28	0.36	0.42	0.46
W 27×84	58.63	336.36	209.26	162.80	141.33	129.65	0.17	0.28	0.36	0.42	0.45
W 30×90	56.41	341.99	213.78	165.05	143.54	130.62	0.17	0.26	0.34	0.39	0.43

Table 7: Comparison of nominal resistance for the limit state of web compression buckling (column webs in moment frames)

Column Sections	P_{nAISC} (kips)	P_{nFEA} (kips) h/b			Ratio = P_{nAISC}/P_{nFEA} h/b		
		10	15	20	10	15	20
W 10×49	130.70	138.82	136.14	134.95	0.94	0.96	0.96
W 12×65	162.00	180.71	177.07	174.82	0.90	0.92	0.92
W 14×61	124.90	176.59	172.31	169.98	0.70	0.72	0.74

Proposed coefficient (k')

To address the shortcoming of the current AISC equations (Eq. 1 and 2) for predicting the limit state of web compression buckling, a new equation is proposed that takes into account the influence of the load bearing length. The format of the proposed equation is expressed by Eq.8. This equation is identical to the elastic buckling equation for a plate, and the coefficient k' takes into account the section depth versus loading bearing length ratio. In this manner the influence of the load bearing width is accounted for while maintaining the origin of the current AISC equations. The coefficient k' was back calculated using Eq. 8, where R_n was taken equal to the computed capacity obtained from finite element analyses. The calculated values for k' are provided in Tables 8 through 10. For interior beam bearing conditions they vary from 2.23 to 4.65, for end bearing conditions they vary from 1.08 to 3.71, and for column sections they vary from 1.31 to 1.78. For h/b ratios higher than and equal to 3.0 the coefficients for end bearing conditions are approximately half of those for interior bearing conditions. As a result, for these cases, a 50% reduction of the buckling capacity of the web for an interior bearing condition would be appropriate to obtain the buckling capacity of the web for an exterior bearing condition. However, for h/b ratios equal to 1.0 and 2.0 the 50% reduction is conservative. The relationship between the k' coefficients for end bearing and interior bearing conditions for h/b ratios equal to 2.0 and 1.0 vary between 63% and 83%, respectively.

$$R_n = k' \frac{\pi^2 E t_w^3}{12(1-\mu^2)h} \tag{8}$$

Table 8: Proposed coefficient (k′) for checking the limit state of web compression buckling (interior beam bearing)

Beam Sections	h/b				
	1	2	3	4	5
W 8×10	3.49	2.69	2.43	2.32	2.23
W 12×16	3.97	3.05	2.76	2.62	2.52
W 16×31	4.47	3.51	3.22	3.08	2.98
W 21×44	4.34	3.35	3.03	2.88	2.77
W 27×84	4.39	3.42	3.13	2.99	2.88
W 30×90	4.65	3.59	3.27	3.11	3.01

Table 9: Proposed coefficient (k′) for checking the limit state of web compression buckling (end beam bearing)

Beam Sections	h/b				
	1	2	3	4	5
W 8x10	2.90	1.74	1.24	1.18	1.08
W 12x16	3.29	1.98	1.54	1.33	1.22
W 16x31	3.59	2.22	1.73	1.52	1.39
W 21x44	3.58	2.18	1.69	1.45	1.33
W 27x84	3.52	2.19	1.70	1.48	1.36
W 30x90	3.71	2.32	1.79	1.56	1.42

Table 10: Proposed coefficient (k′) for checking the limit state of web compression buckling (column webs in moment frames)

Column Sections	h/b		
	10	15	20
W 10×49	1.35	1.32	1.31
W 12x65	1.41	1.38	1.36
W 14x61	1.78	1.73	1.71

5. Conclusions

The current AISC equations for predicting the limit state of web compression buckling do not take into account the influence of the load bearing length. A total of 69 nonlinear finite element analysis were performed to evaluate the accuracy of AISC equations for various loading conditions and to develop a new equation (Eq.8) for predicting the buckling capacity of the web as it relates to the limit state of web compression buckling. The new equation takes into account the influence of the load bearing length through the use of the coefficient k'. The coefficient k' was back calculated from Eq.8 where R_n was taken equal to the peak load obtained from finite element analysis.

It was determined that the current AISC equations (Eq.1 and 2) significantly underestimate the buckling capacity of the web for interior and end bearing conditions for all beam sections considered. This underestimation was more pronounced for low h/b ratios in the beam sections. However, for column sections the buckling capacity of the web calculated based on Equation 1 matched fairly closely with the computed capacities obtained from finite element analyses, especially for W10x49 and W12x65 sections. This observation is consistent with the origin of Equation 1, which was developed to predict the buckling strength of column webs in moment resisting connections. For column section W14x61, Equation 1 underestimated the buckling capacity of the web by 26-30%.

The influence of the load bearing length for the beam sections was more pronounced than in the column sections, because the range of load bearing lengths in the column sections was not as large as the range for the beam sections. The proposed equation (Eq.8) for predicting the buckling capacity of the web is identical to the elastic plate buckling equation, and the coefficient k' takes into account the section depth versus loading bearing length ratio. The values for the coefficient k' for the beam sections varied from 2.23 to 4.65 for interior bearing conditions and from 1.08 to 3.71 for end bearing conditions. For the column sections the coefficient k' varied from 1.31 to 1.78.

Equation 8 together with the k' values provided in this paper can be used to more accurately predict the buckling capacity of the web as it relates to the limit state of web compression buckling.

6. Recommendations for future work

The wide flange section lengths (L) used in this study were taken equal to three times the overall depth of the section (3h) to allow for a sufficient distribution of the applied load to the web of the section. This selection was based on the assumption that if the applied load is distributed at a 45^o angle to the web of the section, the necessary section length to allow this distribution is 2h. Accordingly, a section length equal to 3h was selected to ensure a proper distribution of the applied load to the web of the section even if the distribution took place at angle smaller than 45^o with the horizontal axis. Additionally, the edges of the webs for all wide flange sections were conservatively modeled as free. The influence of greater section lengths and alternative boundary conditions for the edges of the web on the buckling capacity of the web should be investigated. Also, because the peak loads obtained from the nonlinear finite element analyses were achieved after the wide flange sections were compressed past their linear range, the effect that the yield stress has on the peak loads should be examined. Finally, the proposed mathematical model relies on tabulated k' values for predicting the limit the limit state of web compression buckling. These k' values are currently available only for the sections investigated in this study. A generalized mathematical model should be developed that provides a closed from solution for predicting the limit state of web compression buckling and that can be used for any wide flange section.

References

Abaqus User's Manual Version 6.14-2, Dassault Systemes Simulia Corp. (2014).

AISC (2010), "Specification for Structural Steel Buildings", AISC, Chicago, IL.

Arasaratnam, P., Sivakumaran, K. S., & Tait, M. J. (2011), "True stress-true strain models for structural steel elements", International Scholarly Research Notices.

Chen, F. W., Newlin, D. E., "Column Web Strength in Steel Beam-to-Column Connections", ASCE Annual and National Environmental Engineering Meeting October 18-22, 1971, St. Louis, Missouri.

Crisfield, M.A. (1981). ″A fast incremental\iteration solution procedure that handles snapthrough, ″ Computers and Structures, 13, 55-62.

Moen, D.C., (2008),"Direct strength design of cold-formed steel members with perforations", *PhD Dissertation*, John Hopkins University, Baltimore, MD.

Soltani, M. R., Bouchaïr, A., Mimoune, M. (2012), "Nonlinear FE analysis of the ultimate behavior of steel castellated beams", *Journal of Constructional Steel Research*, 70, 101-114.